A Combined Quantum Mechanical/Molecular Mechanical Model of the Potential Energy Surface of Ester Hydrolysis by the Enzyme Phospholipase A_2

Bohdan Waszkowycz,[a] Ian H. Hillier,*[,a] Nigel Gensmantel[b] and David W. Payling[b]
[a] *Department of Chemistry, University of Manchester, Manchester M13 9PL, UK*
[b] *Fisons PLC, Pharmaceuticals Division, Bakewell Road, Loughborough, Leicestershire LE11 0RH, UK*

A combined molecular orbital/molecular mechanical computational model has been developed to study the potential energy surface of catalysis by the enzyme phospholipase A_2. By the integration of molecular mechanical and quantum mechanical forces, the model allows the geometry optimisation of a molecule within a large and complex environment, such as the enzyme active site. The method has been applied to an examination of the role of histidine in the hydrolysis of an ester by phospholipase A_2. Proton transfer to and from the imidazole ring of histidine is shown to be a valid mechanism, in that it occurs with minimal structural change and against a favourable potential energy surface.

In recent years. computational chemistry has made a significant contribution to the understanding of enzyme catalysis. The most successful approaches have involved the combination of empirical force-field methods (*e.g.* molecular mechanics) with quantum mechanical methods, which employ *ab initio* or semi-empirical molecular orbital (MO) schemes. This allows the modelling of macromolecular interactions, for example the fitting of a substrate in the active site, as well as the quantitative treatment of the bond-breaking or bond-forming processes which characterise catalysis.[1]

However, it remains difficult to follow in detail a reaction path within the enzyme active site. Potential energy surfaces which involve electronic rearrangement must be determined quantum mechanically, with the most common strategy being the use of simple models of the active site treated *in vacuo*.[2] Such an approach is often unsatisfactory because, due to computational expense, the quantum mechanical models usually involve only a small number of atoms to represent fragments of a few active site residues. Such models tend to be a poor approximation of the complex steric and electrostatic environment of the protein. These bulk steric and electrostatic interactions are of major importance in the control of the catalytic mechanism, as they are responsible for the correct alignment of reactants and for the stabilisation of high-energy intermediates. As a result, the structure and energy of a transition state obtained *in vacuo* may be significantly different from that occurring *in situ* (*i.e.* in the active site). On a practical point, it may be difficult to optimise a structure *in vacuo* without building into the system an arbitrary set of geometry constraints, to preserve the conformations normally imposed by the environment of the active site.

Refinements to the above method include the use of a field of point charges (partial or integral) to reproduce the electrostatic potential of the bulk protein, or the representation of the dielectric continuum by reaction field methods. The incorporation of point charges into the MO one-electron Hamiltonian is a computationally inexpensive method of representing the polarisation of the wave-function by the bulk enzyme, and has been widely used to account for the long-range electrostatic interactions which are of major importance in enzyme catalysis.[3] In the reaction field method, the substrate is placed within a homogeneous dielectric continuum which is polarised by the substrate.[4] While this can accurately simulate a bulk solvent environment,[5] it is less satisfactory for the heterogeneous environment of the protein. Heterogeneous reaction field methods have recently been developed for application to enzyme catalysis.[6] Although such methods may accurately describe bulk electrostatic and dielectric interactions, they are not appropriate for geometry optimisations because of the neglect of all steric interactions between the quantum mechanical atoms and the environment.

Here we have tried to overcome some of these problems by the use of an integrated quantum mechanical–molecular mechanical methodology, which allows us to model the important residues of the active site as a quantum mechanical (QM) system within a larger molecular mechanical (MM) system which represents the bulk enzyme. Geometry optimisation of the QM system is influenced by electrostatic and steric interactions with the MM atoms. Hence a potential energy surface can be determined, which, to a first approximation, reflects the reaction path *in situ* rather than *in vacuo*.

Such hybrid QM–MM calculations have been proposed by other workers, although none has found widespread use. The earliest combined MM with semi-empirical MO theory (*e.g.* Warshel and Levitt's study of lysozyme[7]), whereas more recently various integrations of MM or molecular dynamics with empirical valence bond[8] or *ab initio* MO[9,10] calculations have been attempted. Our work follows the methodology of Singh and Kollman's program QUEST[9] (part of the AMBER[11] suite), with some minor modifications by us.

We have applied this technique to an investigation of the mechanism of catalysis by the enzyme phospholipase A_2 (PLA2). PLA2 hydrolyses the phospholipids of cell membranes to release fatty acids such as arachidonic acid, and thereby initiates the production of a diverse range of potent cellular mediators such as the prostaglandins.[12] Inhibition of PLA2 is a potentially important route to the treatment of various inflammatory disorders, and therefore an understanding of the mechanism of catalysis may contribute to rational drug design.[13]

A mechanism has been proposed by Verheij *et al.*[14] based on the X-ray crystal structure of PLA2,[15] which shows similarities to that of other hydrolytic enzymes, in particular the serine proteases. As there has been insufficient experimental evidence to date to prove this mechanism, the application of theoretical calculations is a potentially powerful route to explore those details of catalysis which may not be determined readily by experiment.

Our earlier calculations on PLA2 suggested that this mechanism was valid on structural and energetic grounds.[16,17] In this paper we present the example of ester hydrolysis by PLA2 to demonstrate the use of combined QM–MM methods in the determination of a reaction path, by considering the

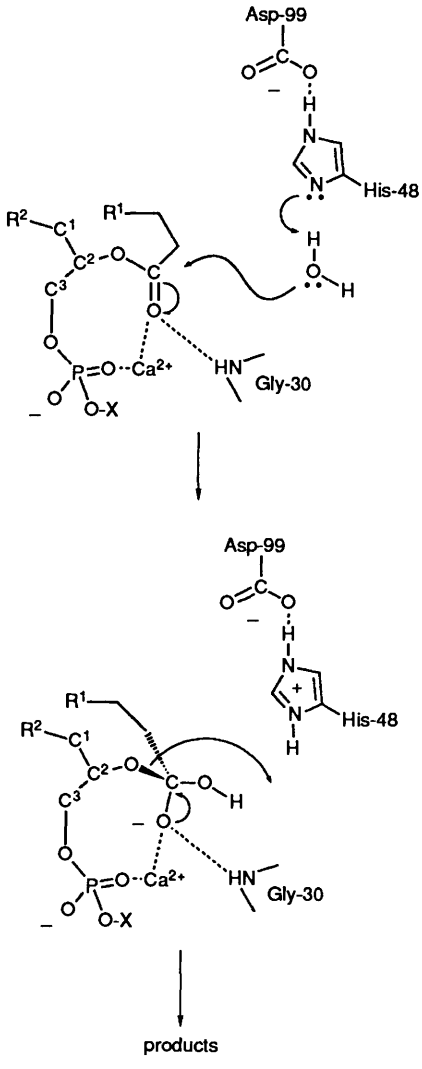

Fig. 1 Proposed mechanism of catalysis by PLA2

formation and breakdown of the tetrahedral oxyanion which is presumed to be an intermediate in ester hydrolysis by PLA2, as well as in hydrolysis by the serine proteases in general.[18]

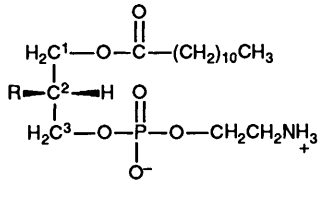

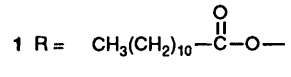

1 R = $CH_3(CH_2)_{10}—C(=O)—O—$

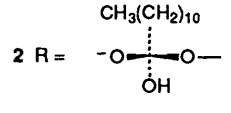

2 R =

The proposed mechanism of catalysis may be described briefly.[14] PLA2 hydrolyses only the 2-acyl ester bond of 1,2-diacyl-*sn*-3-glycerophosphatides (L-α-phospholipids, *e.g.* **1**). A histidine ring (His-48 of bovine pancreatic PLA2) and a calcium ion are known to be essential for activity. The hydrogen-bonded histidine-aspartate couple, found within the hydrophobic wall of the active site cleft, is proposed to function similarly to the serine-histidine-aspartate triad of the serine proteases. In PLA2 a water molecule is assumed to be the active nucleophile in the absence of serine. The phospholipid substrate is presumed to bind to the calcium *via* the C^2 carbonyl and a phosphoryl oxygen, with the acyl chains interacting with the hydrophobic wall (Fig. 1). The polarised carbonyl is attacked by the water molecule (present in the crystal structure of bovine PLA2), with proton transfer to His-48. This results in the formation of a high-energy tetrahedral oxyanion intermediate, which is stabilised by electrostatic interaction with the calcium ion. Proton transfer from His-48 to the C^2 ether oxygen occurs on the breakdown of the intermediate, to release the C^2 fatty acid.

Molecular modelling with molecular mechanics and computer graphics has demonstrated that the phospholipid substrate can be fitted into the active site with minimal distortion of the extended conformation which the substrate adopts in the lipid membrane.[16,17,19] The binding of the C^2 carbonyl oxygen and a phosphoryl oxygen to the calcium ion is presumably responsible for the alignment of the carbonyl with the water-His-Asp system. Our *ab initio* MO calculations, within the program GAMESS,[20] suggested that the oxyanion intermediate can be effectively stabilised by electrostatic interactions both within the calcium-oxyanion-His-Asp system and also between this system and the bulk environment.[16,17] In these calculations the bulk electrostatic interactions were reproduced by the use of a field of point partial charges incorporated into the one-electron Hamiltonian.

Our previous work concentrated on only two points on the potential energy surface, the reactants and the oxyanion intermediate, where the latter was assumed to occupy a shallow minimum on the potential energy surface between the transition states which lead to its formation and breakdown. Here we take the opportunity to examine the reaction path in more detail, in order to model a series of structures, optimised *in situ* by the combined QM–MM method, which follow the important step of proton transfer from the attacking water to the imidazole ring, and thence to the alkoxy leaving-group. This role of histidine as both a proton acceptor and donor is central to the catalytic mechanism of many other enzymes, and hence our results have implications beyond PLA2.

Computational Method.—The initial MM modelling of PLA2 is fully described in our earlier papers.[16,17] In brief, we have used the program AMBER to build and minimise structures of a phospholipid substrate (1,2-dilauryl-3-*sn*-phosphatidylethanolamine, **1**) within the active site of PLA2. No X-ray structures are available for such a complex, and therefore the substrate was modelled in the extended conformation reported to be present in the lipid membrane,[21] and fitted into the known crystal structure of the uncomplexed bovine pancreatic PLA2.[15] The oxyanion **2** which is presumed to be the intermediate formed on the hydrolysis of **1** was also modelled. For these MM minimisations the entire enzyme (123 amino acid residues) was treated. To the 106 water molecules present in the X-ray structure were added a further 640 in order to produce a complete solvation shell around the enzyme. A united-atom force-field[22] was used for the bulk of the system, with an all-atom force-field[23] for the active site and the substrates. The MM force-field geometries for the oxyanion were taken from QM optimisations of model oxyanions, with partial charges determined by the electrostatic potential method of Singh and Kollman,[24] with an STO-3G basis set.

A small constraint was employed during minimisation of the oxyanion to ensure that the C^2 alkoxy oxygen was positioned close to His-48, in order to achieve the doubly hydrogen-bonded structure in Fig. 2. As will be seen later, small oxyanions achieve this conformation readily, which suggests that the full-sized phospholipid is prevented from doing so only by a local

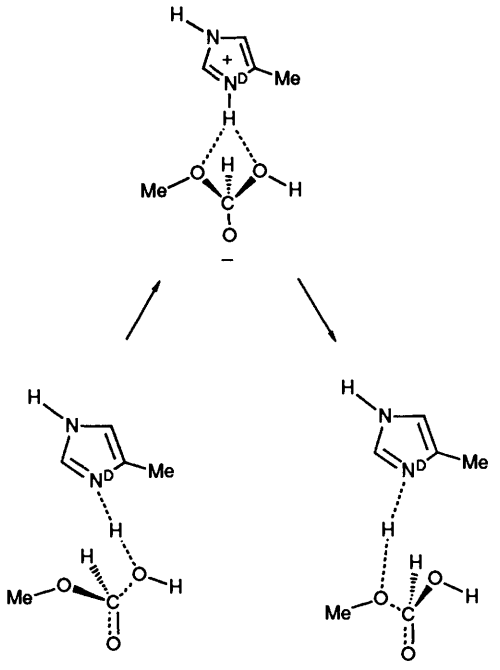

Fig. 2 Quantum mechanical system considered in the calculations. The attack of water on methyl formate leads to the formation of the doubly hydrogen-bonded intermediate.

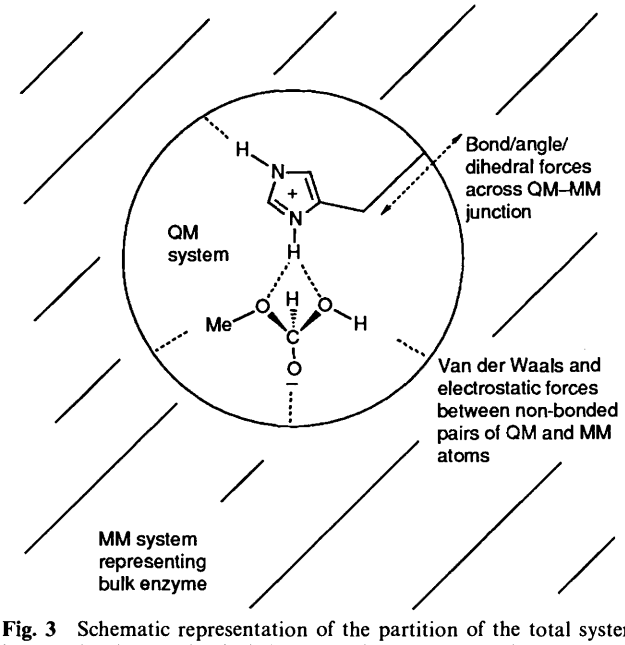

Fig. 3 Schematic representation of the partition of the total system into molecular mechanical (MM) and quantum mechanical (QM) fragments. The MM system consists of *ca.* 200 atoms.

conformational energy barrier. In the absence of this doubly hydrogen-bonded structure, it is difficult to envisage the facile transfer of the proton from N^D of His-48 to the alkoxy oxygen. (A similar structure is proposed for hydrolysis by the serine protease.[18]) A fuller description of the MM-minimised PLA2-oxyanion structure is given in ref. 17.

For the QM–MM optimisations, a small active site model was produced, which consisted of *ca.* 200 atoms (17 amino acid residues, the calcium ion and four water molecules within the active site), as in Plate 1. A small substrate (methyl formate) was used instead of the full-sized phospholipid (with a separate residue to represent the phosphoryl ethylammonium side-chain). The QM atoms of this system were defined as the whole of the oxyanion and the imidazole ring (plus β-methylene) of His-48 (Fig. 2); all other atoms were treated by MM. (Note that the valency of the β-methylene fragment is filled by the addition of a hydrogen atom in the QM calculation.) The QM–MM optimisation involved a standard *ab initio* geometry optimisation of the QM system, which also incorporated MM gradients from the surrounding MM atoms. This was achieved by the addition of the MM gradients (exerted by the MM atoms on the QM atoms) to the QM gradients of the QM atoms.[9] Note that during the optimisation of the QM atoms, the MM system is static (but may itself be refined by MM once QM optimisation is complete).

The MM forces comprise both bonded and non-bonded terms (Fig. 3). Thus, the His-48 β-carbon is considered to be attached to the MM α-carbon *via* an MM bond. Across this QM–MM junction, the ring feels standard MM bond/angle/dihedral forces between appropriate pairs of atoms. The non-bonded MM forces consist of the standard AMBER 6-12 Lennard–Jones potential, which is replaced by a 10-12 potential for hydrogen-bonded pairs.[22,23]

Electrostatic interactions between QM and MM atoms are described by the incorporation into the one-electron Hamiltonian of the point charges of all MM atoms (except the His-48 α-carbon, which would otherwise be very close to the QM β-hydrogens). This allows the wave-function of the QM system to be polarised by the field of charges, to mimic the polarisation of the system within the enzyme. Note that the oxyanion is not bonded to the MM system, and hence experiences only MM van der Waals forces as well as the above electrostatic interactions. The junction hydrogen, which is added to fill the valency of the QM system, interacts only with the other QM atoms and the point charge field, and feels no MM forces.

The end result is that a QM optimisation can be performed which, to a first approximation, simulates the system *in situ*. A practical benefit is that no arbitrary constraints need to be imposed to maintain the conformation of the QM system. We have not found any stable dimer during our attempts to optimise the imidazolium–oxyanion couple *in vacuo* using QM alone. In our QM–MM model, the dissociation of the dimer is prevented by the MM forces which simulate interaction with the active site. Thus the imidazole ring is restricted in its movement *via* the forces which connect it to the MM atoms, as well as by van der Waals forces to its non-bonded neighbours, while the mobility of the oxyanion is limited only by non-bonded forces. A small oxyanion was chosen (rather than a full phospholipid) so as not to restrict its freedom of movement within the active site. Had it been a full-sized phospholipid, treated partly as QM, partly MM, the QM system would have had limited mobility because of the MM bond forces which would attach it to the stationary MM atoms.

In practice, the imidazolium–oxyanion system was fully optimised at a 3-21G basis set (123 basis functions). The only constraints imposed were to freeze in space the imidazole β-carbon and to prevent out-of-plane movement of the imidazole ring. These constraints are not strictly necessary, since the MM forces serve to limit the movement of the ring. They were employed here to hasten the convergence of the optimisation, which may otherwise be severely hampered by small out-of-plane movements of the imidazole ring.

Optimisation of the oxyanion–imidazole system resulted in the structure described in Figs. 4 and 5. This was used to generate a series of intermediate structures along the reaction surface, by means of re-optimising the QM system for specific stretches of either the C–OH bond (to model the surface towards the reactants, HCOOMe + HOH) or the C–OMe bond (to model the formation of the products, HCOOH + MeOH). With the C–OH and C–OMe bonds being of lengths 1.461 and 1.477 Å, respectively, in the fully optimised structure,

Table 1 Selected geometries for the imidazole–oxyanion series of structures. Model MIN is the fully optimised structure, whereas models R1–R5 and P1–P5 represent movement towards reactants or products respectively. Thus the C–OH bond ranges from 1.55 Å in model R1 to 2.0 Å in model R5. R5 and P5 represent the extremes of reactants and products. For atom labels see Fig. 5

	Length/Å						Angle/°	Dihedral angle/°
Model	C–O^H	C–O^M	C–O	H^T–N^D	H^T–O^H	H^T–O^M	H^T–N^D–C^G	H^T–N^D–C^G–C^D
R5	2.00	1.335	1.243	1.572	1.021	—	111.7	172.4
R4	1.85	1.355	1.256	1.491	1.052	—	114.8	172.6
R3	1.75	1.393	1.279	1.101	1.419	—	119.4	173.7
R2	1.65	1.414	1.292	1.069	1.501	—	120.2	173.1
R1	1.55	1.451	1.304	1.039	1.656	—	122.1	172.5
MIN	1.461	1.477	1.312	1.023	1.861	2.019	124.6	172.1
P1	1.424	1.55	1.305	1.045	—	1.622	130.5	171.9
P2	1.407	1.65	1.291	1.057	—	1.559	131.8	172.7
P3	1.390	1.75	1.279	1.074	—	1.496	132.9	173.8
P4	1.356	1.85	1.255	1.494	—	1.053	139.8	167.5
P5	1.338	2.00	1.242	1.579	—	1.023	142.6	164.1

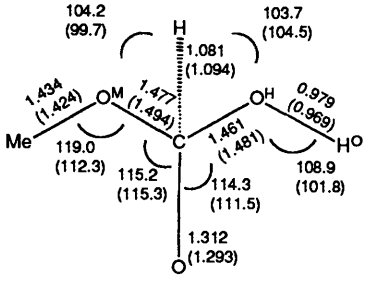

Angles /°

H–C–O	116.2	(119.8)
O^M–C–O^H	101.5	(104.3)

Dihedral angles/°

Me–O^M–C–O^H	−126.3	(−80.8)
Me–O^M–C–O	−2.3	(41.8)
Me–O^M–C–H	126.1	(171.5)
O^M–C–O^H–H^O	90.8	(119.2)
O–C–O^H–H^O	−33.9	(−5.8)

Fig. 4 Comparison of the geometry of the oxyanion optimised *in situ* (parameters without parentheses) and *in vacuo* (within parentheses). Length/Å; angle/°.

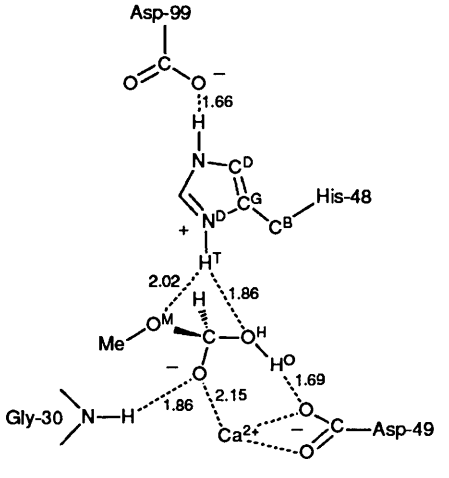

Fig. 5 Selected intermolecular geometries for the doubly hydrogen-bonded oxyanion, optimised within the active site model. Length/Å.

the intermediate structures were generated for lengths of 1.55, 1.65, 1.75, 1.85 and 2.0 Å, to model bond stretches of up to *ca.* 0.5 Å from the optimised geometry, in order to follow the transfer of the proton to and from the imidazole ring. Thus a sequence of ten structures was generated in which all geometric parameters of the QM system, except for either the C–OH or C–OMe lengths, were fully optimised.

As the active site environment for this QM–MM system was fairly limited, the structures were later built into a more extensive active site model which was derived from the MM-minimised PLA2-oxyanion system.[17] This comprised *ca.* 1000 atoms (68 amino acid residues, 50 water molecules). In this model the aspartate side-chain of Asp-99 was also treated quantum mechanically (as an acetate molecule). Single-point calculations for the 11 optimised structures were performed using a 4-31G basis set in the program GAMESS, both for the QM system *in vacuo* as well as with the extensive field of charges included in the Hamiltonian.

Results and Discussion

The geometries of the various oxyanion–imidazolium systems are described in Figs. 4 and 5 and Table 1, and are shown in Plate 2. The structure of the oxyanion which is obtained *in situ* (by the combined QM–MM method) is very similar to that obtained *in vacuo*, although the geometry is to some extent influenced by the active site; for example, the calcium ion causes some stretch of the C–O bond, and the position of H^O is influenced by the hydrogen bond with the carboxylate of Asp-49, one of the ligands of calcium. The position of the oxyanion within the active site demonstrates that it forms the doubly hydrogen-bonded structure readily, and is held in place solely by the hydrogen bonds to His-48 and Asp-49, and the electrostatic interaction with the calcium ion.

Proton transfer from water to imidazole is seen to be complete before transfer occurs from imidazole to the methoxy residue. This transfer relies only on the opening-up of the angle which the proton makes to the imidazole ring, and does not require any movement of the ring itself, which is static during the sequence of structures. (Note that the internal geometry of the ring was allowed to change during optimisation.) Again, there is comparatively little movement of the substrate over the reaction path: the substrate pivots on the carbonyl oxygen, moving slightly closer to the calcium as the full charge develops on the oxyanion. Thus the reaction is seen to involve the movement of the substrate into the active site and towards the stationary water molecule, which is held in place by hydrogen bonds to His-48 and Asp-49.

The QM energies of these structures are presented in Figs. 6 and 7. The 3-21G energies (Fig. 6) have been taken directly from the QM–MM optimisations in the small active system. ΔE_{MM} is the MM energy of interaction between the MM and QM atoms,

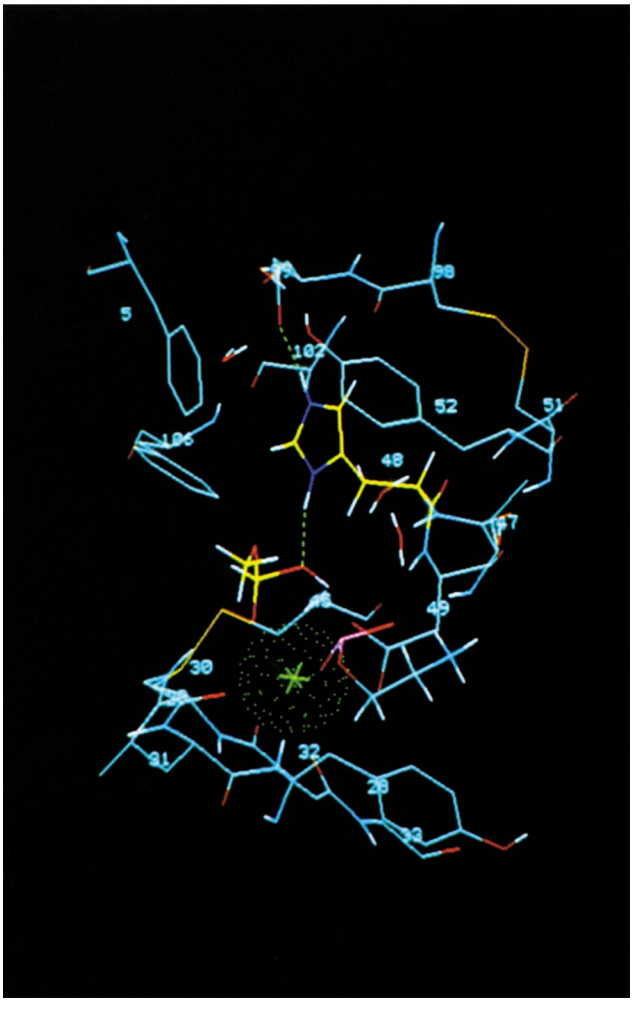

Plate 1 The structure of the MM model of the active site of PLA2 used for the QM–MM optimisations. The oxyanion and His-48 are highlighted by the use of yellow carbon atoms. The green dot surface represents the calcium ion.

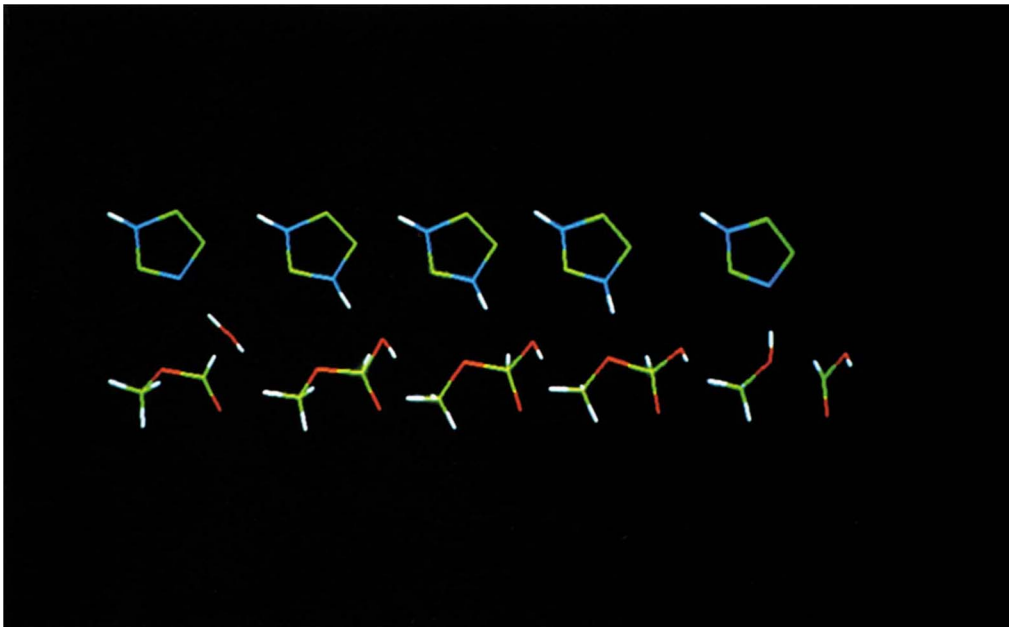

Plate 2 A sequence of structures from the QM–MM optimisation of the oxyanion–imidazolium couple in the active site of PLA2. From left to right, the five structures represent the following models (described in Table 1): R5 (the reactants); R3; MIN (the fully optimised oxyanion); P3; and P5 (the products).

(Facing p. 228)

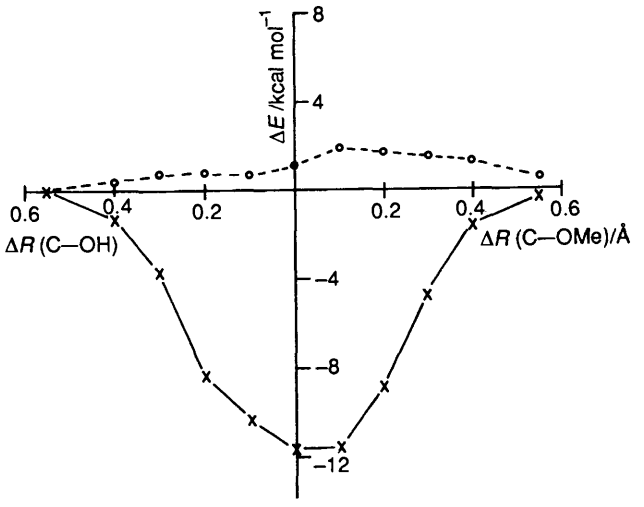

Fig. 6 The *in situ* potential energy surface for ester hydrolysis within the small active site model. The solid curve represents ΔE_{tot} and the dashed curve ΔE_{MM}, where ΔE_{tot} is the sum of ΔE_{QM} and ΔE_{MM}. ΔR is the stretch of the C–OH or C–OMe bond, where the origin represents the fully optimised structure (denoted as MIN in Table 1). Points to the right of the origin represent C–OMe stretch (*i.e.* towards products) and points to the left of the origin represent C–OH stretch (*i.e.* towards reactants). E_{QM} evaluated with the 3-21G basis set.

and hence reflects mainly the increase in van der Waals repulsion, of the order of 1 kcal mol^{-1}, as the substrate moves into the active site to form the oxyanion. (Absolute E_{MM} for the oxyanion–imidazole system is −7.4 kcal mol^{-1}, which is predominantly $E_{van\ der\ Waals}$, with E_{H-bond} of −0.4 kcal mol^{-1}.) ΔE_{tot} is the sum of ΔE_{MM} and ΔE_{QM}, and shows a significant minimum (12 kcal mol^{-1}) to the formation of the oxyanion, while reactants and products are of similar energy.

The upper curve in Fig. 7 is ΔE_{QM}, calculated using a 4-31G basis set, for the series of oxyanion–imidazolium structures evaluated *in vacuo*. As may be expected, there is a large barrier to the formation of the oxyanion. The plot shows the two slight peaks associated with the two transition states, although this may be to some extent fortuitous in view of the accuracy of the 4-31G basis set. The lower curve of Fig. 7 shows ΔE_{QM} for the reaction in the large active site model, with the acetate side-chain of Asp-99 also treated as QM, and again shows the marked minimum. It can be seen that proton transfer to and from the imidazole occurs for a C–OH and C–OMe bond length in the range 1.75–1.85 Å. Both regions correspond to large energy changes for the *in vacuo* calculations and quite small energy changes for the *in situ* model, which is a consequence of the stabilisation which results from the interaction with the MM system.

There are several reasons why the potential energy surface might show a minimum *in situ*. Firstly, although the 4-31G basis set predicts proton affinities for these systems with reasonable accuracy,[2c] the omission of electron correlation is expected to be a source of error. Our earlier calculations on small model systems demonstrated that the 4-31G basis will underestimate the barrier to ester hydrolysis (at least by *ca.* 10 kcal mol^{-1}) when compared with the 6-31G** basis set with electron correlation estimated at the MP2 level.[17] Thus the *in situ* reaction surface would be expected to appear much shallower if evaluated at this level of theory. Secondly, the point charge model is of necessity approximate and may give rise to an exaggerated minimum, since the use of static charges does not allow for the polarisation of the MM environment by the QM atoms, which may be significant in shielding the charge which arises on the oxyanion and imidazolium.

Even so, ΔE_{QM} may still show a small minimum *in situ*, which would serve to negate any barrier in ΔE_{MM}. Our ΔE_{MM} is small,

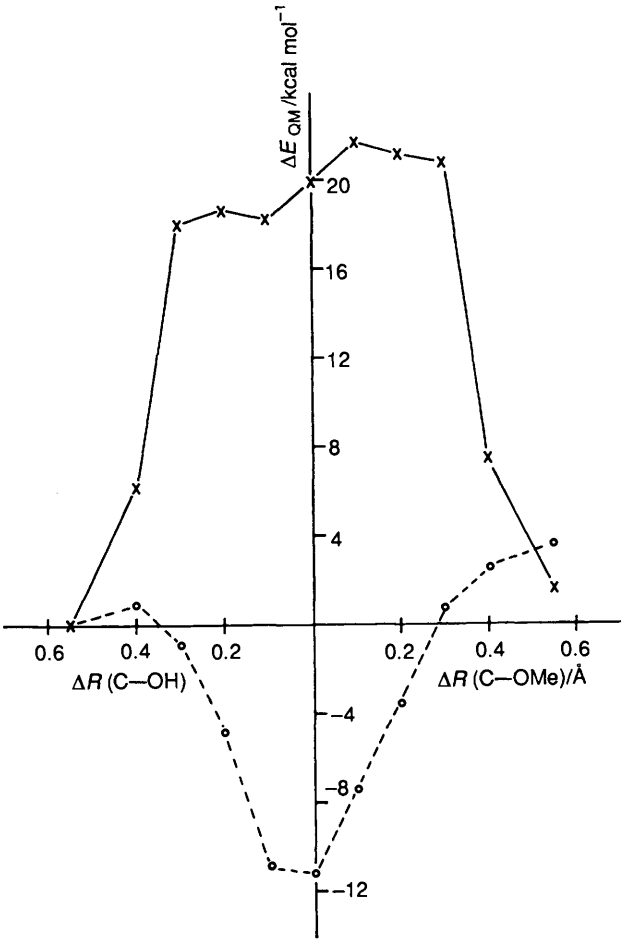

Fig. 7 The *in vacuo* and *in situ* potential energy surfaces for ester hydrolysis. The *in vacuo* surface (solid curve) represents ΔE_{QM} for the oxyanion and imidazolium alone, while the *in situ* surface (dashed curve) represents ΔE_{QM} for the oxyanion–imidazolium–acetate system (the latter representing Asp-99) within the extended active site environment. E_{QM} evaluated with the 4-31G basis set.

Table 2 Selected 4-31G Mulliken populations for models R5, MIN and P5 (see Table 1), determined both *in vacuo* and *in situ* (*i.e.* in the extended field of charges, and with Asp-99 represented explicitly by acetate)

	in vacuo			*in situ*		
Atom	R5	MIN	P5	R5	MIN	P5
C	+0.76	+0.75	+0.75	+0.86	+0.82	+0.83
O	−0.70	−0.82	−0.68	−1.00	−1.12	−0.97
O^H	−0.92	−0.79	−0.76	−0.96	−0.85	−0.76
O^M	−0.74	−0.85	−0.89	−0.71	−0.83	−0.90
N^D	−0.78	−0.93	−0.78	−0.84	−0.97	−0.84

simply because we have looked at a small oxyanion within a small active site model. As discussed previously, when a full-sized phospholipid forms an oxyanion there is some increase in torsional E_{MM} within the substrate, as well as a larger $E_{van\ der\ Waals}$.[17] Thus a larger barrier in ΔE_{MM} would be expected, compared to that observed here.

Table 2 presents Mulliken populations obtained *in vacuo* and *in situ*. These demonstrate the role of the environment, and in particular the calcium ion, in the polarisation of the substrate carbonyl, which presumably assists nucleophilic attack by the water molecule. There is also significant polarisation of the water molecule and the imidazole ring *in situ*.

It should be stressed that the sequence of structures obtained here is strictly relevant only to the computational model employed. Thus, the use of a different basis set or field of charges would produce a somewhat different potential energy surface. For example, a change in the basis set or the field of charges may stabilise the ionic oxyanion–imidazolium in preference to the neutral ester–water–imidazole, and thus one might find that the point at which the proton transfers from oxyanion to imidazole is altered. However, the potential energy surface should remain essentially the same. The well-depth observed here is similar to that we obtained in our earlier work, though it should be noted that here we have not looked at the full potential energy surface but only at a maximum separation of reactants (or products) of 2 Å. The earlier work used a larger oxyanion and allowed for minimisation of the MM atoms around both substrate and oxyanion. Here the use of a small oxyanion will result in the loss of some torsional energy in E_{QM}, as well as the inclusion of a few extra point charges in the environment. A more significant effect may be due to the use of the same MM structure throughout the sequence of QM structures, such that the MM atoms are prevented from adapting to changes in the conformation and charge of the QM atoms. Thus it must be said that at best only semi-quantitative comparisons can be made between calculations which do not use exactly the same field of charges.

In conclusion, it should be noted that these calculations are strictly an investigation of the hydrolysis of a small ester, methyl formate, in PLA2, and not a full-size phospholipid substrate. A phospholipid can be modelled in an identical manner, except that the phospholipid itself would be divided into QM and MM fragments. As the MM environment is held static during QM optimisation, the QM part of the lipid would have limited mobility in the active site. Therefore the full reaction surface could not be obtained without the entire lipid being repositioned at each step, which would necessarily bias the optimisation of the QM system. The purpose of our choice of a small substrate was to demonstrate that, even when there are no MM bonds to hold the oxyanion in place, the oxyanion will adopt a reasonable position, which is dependent only on the balance of QM interactions (with imidazole and the field of charges) and MM interactions (with the environment, *via* van der Waals forces). As a result, the small oxyanion may have more mobility than would be experienced by the phospholipid. However, the final structures of reactants and products do not look unrealistic.

Conclusions

The purpose of these calculations is to demonstrate the potential of combining QM and MM forces in order to attempt to optimise a structure quantum mechanically within a bulk environment. The advantages of the technique are twofold. From a theoretical view, changes in structure which occur *in situ* due to electrostatic and steric interactions can be investigated. Although this may be done to some extent with MM alone for structures which occupy potential energy minima, MM becomes inadequate for structures in which bonds are being broken and formed. Here an MO method is needed to evaluate these transition structures, while MM forces are adequate to describe the interactions with the bulk environment.

On a practical point, the method allows the investigation of supermolecule geometries which may be impossible to obtain by QM alone, unless a large number of geometric constraints are imposed in order to maintain desired conformations. This is true in the calculations reported here, where the oxyanion–imidazolium couple is held in place solely by the active site environment. Thus, no arbitrary constraints are imposed which might bias the route of optimisation. The method can be extended to locate transition states, although the potential energy surface *in situ* is a simple minimum for the system studied here.

The calculations represent a fairly simple model of a reaction path, and have a number of sources of error. Clearly, a higher level of MO theory (larger basis sets, with electron correlation) would be desirable, as would the inclusion of more QM atoms, but at present such improvements are prohibitively expensive in computational resources. More realistic perhaps would be improvements in the MM system, with the use of polarisable charges, or a method of optimising both QM and MM atoms simultaneously. Thus our methodology is not intended to be the final word in the integration of QM and MM theory.

Finally, one should comment on the relevance of this work to PLA2 and to similar enzyme mechanisms. Our calculations have been designed to investigate the validity of the proposed mechanism of action of PLA2 by consideration of both the macromolecular structures of PLA2-phospholipid complexes (in the absence of crystallographic data) as well as the energetics of phospholipid hydrolysis. This work has concentrated on the reaction path of ester hydrolysis, in order to demonstrate that the proton transfer from the water molecule *via* His-48 to the alkoxy oxygen can proceed readily, with insignificant structural distortion (*i.e.* of His-48 or the substrate) and over a favourable potential energy surface. This is further evidence which is in agreement with the proposed mechanism.

Acknowledgements

This work was supported by the SERC under grants GR/E53682 and GR/F49934.

References

1 (*a*) G. Bolis, M. Ragazzi, D. Salvaderi, D. R. Ferro and E. Clementi, *Gazz. Chim. Ital.*, 1978, **108**, 425; (*b*) G. Alagona, P. Desmeules, C. Ghio and P. A. Kollman, *J. Am. Chem. Soc.*, 1984, **106**, 3623; (*c*) S. J. Weiner, G. L. Seibel and P. A. Kollman, *Proc. Natl. Acad. Sci. USA*, 1986, **83**, 649.
2 (*a*) R. Broer, P. T. van Duijnen and W. C. Nieuwpoort, *Chem. Phys. Lett.*, 1976, **42**, 525; (*b*) S. Nakagawa, H. Umeyama and T. Kudo, *Chem. Pharm. Bull.*, 1980, **28**, 1342; (*c*) P. A. Kollman and D. M. Hayes, *J. Am. Chem. Soc.*, 1981, **103**, 2955.
3 (*a*) D. M. Hayes and P. A. Kollman, *J. Am. Chem. Soc.*, 1976, **98**, 7811; (*b*) L. C. Allen, *Ann. NY. Acad. Sci.*, 1981, **367**, 383; (*c*) S. Nakagawa and H. Umeyama, *J. Theor. Biol.*, 1982, **96**, 473; (*d*) S. Nakagawa and H. Umeyama, *J. Mol. Biol.*, 1984, **179**, 103.
4 O. Tapia and O. Goscinski, *Mol. Phys.*, 1975, **29**, 1653.
5 (*a*) M. K. Karelson, A. R. Katritzky, M. Szafran and M. C. Zerner, *J. Org. Chem.*, 1989, **54**, 6030; (*b*) M. Karelson, T. Tamm, A. R. Katritzky, M. Szafran and M. C. Zerner, *Int. J. Quantum Chem.*, 1990, **37**, 1.
6 (*a*) B. T. Thole and P. T. van Duijnen, *Theor. Chim. Acta (Berlin)*, 1980, **55**, 307; (*b*) O. Tapia and G. Johannin, *J. Chem. Phys.*, 1981, **75**, 3624; (*c*) J. A. C. Rullman, M. N. Bellido and P. T. van Duijnen, *J. Mol. Biol.*, 1989, **206**, 101.
7 A. Warshel and M. Levitt, *J. Mol. Biol.*, 1976, **103**, 227.
8 (*a*) A. Warshel and R. M. Weiss, *J. Am. Chem. Soc.*, 1980, **102**, 6218; (*b*) A. Warshel and F. Sussman, *Proc. Natl. Acad. Sci. USA*, 1986, **83**, 3806; (*c*) J. Åqvist and A. Warshel, *Biochem.*, 1989, **28**, 4680.
9 U. C. Singh and P. A. Kollman, *J. Comput. Chem.*, 1986, **7**, 718.
10 J. Chandrasekhar, S. F. Smith and W. L. Jorgensen, *J. Am. Chem. Soc.*, 1985, **107**, 154.
11 P. K. Weiner and P. A. Kollman, *J. Comput. Chem.*, 1981, **2**, 287.
12 A. J. Slotboom, H. M. Verheij and G. H. de Haas, *New Comprehensive Biochemistry*, 1982, **4**, 354.
13 J. Chang, J. H. Musser and H. McGregor, *Biochem. Pharmacol.*, 1987, **36**, 2429.
14 H. M. Verheij, J. J. Volwerk, E. H. Jansen, W. C. Puyk, B. W. Dijkstra, J. Drenth and G. H. de Haas, *Biochemistry*, 1980, **19**, 743.
15 B. W. Dijkstra, K. H. Kalk, W. G. J. Hol and J. Drenth, *J. Mol. Biol.*, 1981, **147**, 97.
16 B. Waszkowycz, I. H. Hillier, N. Gensmantel and D. W. Payling, *J. Chem. Soc., Perkin Trans. 2*, 1989, 1795.

17 B. Waszkowycz, I. H. Hillier, N. Gensmantel and D. W. Payling, *J. Chem. Soc., Perkin Trans. 2*, 1990, 1259.
18 (*a*) A. A. Kossiakof and S. A. Spencer, *Biochemistry*, 1981, **20**, 6462; (*b*) T. A. Steitz and R. G. Shulman, *Annu. Rev. Biophys. Bioeng.*, 1982, **11**, 419.
19 M. M. Campbell, J. Long-Fox, D. J. Osguthorpe, M. Sainsbury and R. B. Sessions, *J. Chem. Soc., Chem. Commun.*, 1988, 1560.
20 M. F. Guest and J. Kendrick, GAMESS User Manual, CCP1/86/1, Daresbury Laboratory, UK, 1986.
21 P. B. Hitchcock, R. Mason, K. M. Thomas and G. G. Shipley, *Proc. Natl. Acad. Sci. USA*, 1974, **71**, 3036.
22 S. J. Weiner, P. A. Kollman, D. A. Case, U. C. Singh, C. Ghio, G. Alagona, S. Profeta and P. Weiner, *J. Am. Chem. Soc.*, 1984, **106**, 765.
23 S. J. Weiner, P. A. Kollman, D. T. Nguyen and D. A. Case, *J. Comput. Chem.*, 1986, **7**, 230.
24 U. C. Singh and P. A. Kollman, *J. Comput. Chem.*, 1984, **5**, 129.

Paper 0/03673K
Received 9*th August* 1990
Accepted 4*th October* 1990